

# Incorporating a 3D point source in the ISS FSME for a 1D subsurface and its influence on the subsequent processing

Xinglu Lin\* and Arthur B. Weglein, *M-OSRP/Physics Dept./University of Houston*

## SUMMARY

Based on the current 3D inverse-scattering-series (ISS) free-surface-multiple-elimination (FSME) algorithm (Carvalho, 1992; Weglein et al., 1997, 2003) that was developed for a 3D point source and 3D earth, this paper derives an ISS FSME algorithm that retains the dimension of the source (i.e., 3D point source) and reduces the subsurface dimension from 3D to 1D. Applying this modified algorithm will accurately predict both the phase and the amplitude of the free-surface multiples in seismic data that are generated by a 3D point source and 1D earth (e.g., Central North Sea), compared to the frequently applied 1.5D ISS FSME algorithm that assumes a 2D line source and 1D earth. Numerical tests are performed on 3D source synthetic data sets from a 1D subsurface, to examine the significance of incorporating 3D source in FSME algorithm and the impact of FSM residues on the subsequent ISS internal multiple attenuation. The results demonstrate that the 3D source/1D subsurface ISS FSME algorithm can accurately remove the FSM events in 3D source data. This successful removal of free-surface multiples provides an essential prerequisite for subsequent processing (e.g., internal-multiple attenuation/elimination).

## INTRODUCTION

Multiple removal is a long-standing and challenging task in seismic data processing, which impacts the subsequent imaging and inversion procedures. Many efforts have been made to attenuate or eliminate the free-surface multiples (events that have experienced at least one downward reflection at the air-water surface) in data (e.g., Verschuur et al., 1992; Carvalho, 1992; Weglein et al., 1997, 2003; Weglein and Dragoset, 2008). Among these methods, the inverse scattering series (ISS) free-surface-multiple-elimination (FSME) algorithm provides a multidimensional procedure that eliminates all free-surface multiples (Carvalho, 1992; Weglein et al., 1997, 2003) through a simple subtraction. The Carvalho et al. ISS FSME algorithm has its strengths in that it does not require subsurface information, and it can provide the accurate time and amplitude of all free-surface multiples. However, other approaches, such as the SRME method, often adopt adaptive subtraction with certain criteria (e.g., energy minimization) to eliminate the free-surface multiples, because the SRME method provides approximate amplitude and time of free-surface multiples. Adaptive subtraction works well at times when the events are isolated, however, it can generate issues when the free-surface multiples and primaries are proximal or interfering. The reason is that energy minimization assumes a minimized/decreased energy in data after multiple subtraction, which can be invalid when the energy can increase after removing destructively overlapping free-surface multiples. In other words, for a complex ge-

ology, there is a need for accurate free-surface-multiple predictions of both time and amplitude, where the adaptive subtraction can fail.

As we mentioned above, the ISS FSME algorithm is a multidimensional procedure that can completely remove the free-surface multiples from data without knowing any subsurface information. If we consider a 3D point source as the real source dimension, the complete 3D ISS FSME algorithm, which assumes a 3D point source and a 3D subsurface, can successfully predict both accurate time and amplitude of all free-surface multiples with a complete dataset (requires areal coverage of sources and for each source requires the areal coverage of receivers). Even though the 3D ISS FSME algorithm is a complete and accurate method, there are reasonable circumstances that require less data and less computational cost, for instance, when the earth property only varies in 1D. For a typical pre-stack shot gather coming from a 1D subsurface, the 1.5D ISS FSME algorithm is frequently and naturally applied to predict free-surface multiples (Carvalho, 1992). Since the 1.5D ISS FSME algorithm is derived from a 2D line source ISS FSME algorithm for a 1D subsurface, it can only provide the accurate phase and amplitude of free-surface multiples generated by a 2D line source, rather than a 3D point source. When the data is generated by a 3D point source and a 1D subsurface, this 1.5D algorithm can produce issues and even fail to effectively eliminate the free-surface multiples. Therefore, for field data it is important to incorporate the 3D source dimension for accurate multiple prediction.

This paper will focus on the specific problem of a 3D source/1D subsurface ISS FSME algorithm by reducing a complete 3D ISS FSME algorithm. The reduced algorithm preserves the real 3D source dimension and demands only one pre-stack shot gather for the 3D source data coming from a 1D earth. The numerical tests are performed on 3D source data sets. The results evaluate the significance of incorporating a 3D source in a 1D ISS FSME algorithm by comparing with a frequently used 2D line source/1D subsurface ISS FSME algorithm and showing its impact on the subsequent processing for 3D source data.

## 3D AND 2D ISS FSME ALGORITHM

The preparation of the 3D FSME algorithm starts from data  $D(x_g, y_g, \epsilon_g, x_s, y_s, \epsilon_s; t)$ , where  $(x_g, y_g, \epsilon_g)$  and  $(x_s, y_s, \epsilon_s)$  are the receiver- and source-location, respectively. In addition, the preprocessing - including reference wave-field removal, deghosting and wavelet estimation - needs to be achieved before the ISS free-surface multiple prediction. The preprocessed data are represented by  $D'$ . The 3D source ISS free-surface

## Incorporating a 3D point source in the ISS FSME for a 1D subsurface and its influence on the subsequent processing

multiple elimination algorithm can be written as

$$D'_n(k_{xg}, k_{yg}, k_{xs}, k_{ys}; \omega) = \frac{1}{2i\pi^2 \rho_r B(\omega)} \int_{-\infty}^{\infty} \int_{-\infty}^{\infty} dk_x dk_y D'_1(k_{xg}, k_{yg}, k_x, k_y; \omega) \times q D'_{n-1}(k_x, k_y, k_{xs}, k_{ys}; \omega) e^{iq(\varepsilon_g + \varepsilon_s)}, \quad (1)$$

for  $n \geq 2$  and

$$D'(k_{xg}, k_{yg}, k_{xs}, k_{ys}; \omega) = \sum_{n=1}^{\infty} D'_n(k_{xg}, k_{yg}, k_{xs}, k_{ys}; \omega). \quad (2)$$

$D'$  contains only the deghosted primaries and internal multiples.  $B(\omega)$  and  $\rho_r$  are the source signature and reference medium density, respectively. The vertical wavenumber is defined by  $q = \sqrt{(\frac{\omega}{c_0})^2 - k_x^2 - k_y^2}$ . The 3D algorithm in equations (1) and (2) assumes that the acquisition applies 3D sources and 3D receivers for a 3D subsurface.

Similarly, a set of 2D data  $D(x_g, x_s; t)$  can be transformed into wavenumber-frequency domain and deghosted as  $D'(k_g, k_s; \omega)$ . The 2D ISS free-surface-multiple-elimination algorithm is,

$$D'_n(k_g, k_s; \omega) = \frac{1}{i\pi \rho_r B(\omega)} \int_{-\infty}^{\infty} dk D'_1(k_g, k; \omega) q D'_{n-1}(k, k_s; \omega) e^{iq(\varepsilon_g + \varepsilon_s)}, \quad (3)$$

for  $n \geq 2$  and

$$D'(k_g, k_s; \omega) = \sum_{n=1}^{\infty} D'_n(k_g, k_s; \omega), \quad (4)$$

where the vertical wave-number is  $q = \sqrt{(\frac{\omega}{c_0})^2 - k^2}$ . In contrast to the 3D case, the algorithm in equations (3) and (4) assumes a 2D subsurface, in which the acquisition corresponds to 2D line sources and 2D line receivers.

### THE ISS FSME ALGORITHM ASSUMING A 2D LINE SOURCE FOR A 1D SUBSURFACE

In developing the algorithm for 1D earth pre-stack data, it was natural that people started with the 2D line source ISS FSME algorithm and then reduced it for 1D subsurface data. The data that occurs in the 2D earth can be written as  $D(x_g, x_s; \omega)$  or  $D(x_m, x_h; \omega)$  in the space-frequency domain, where  $x_m = x_g + x_s$  and  $x_h = x_g - x_s$ . The data from a 1D earth, shown as  $D^{2D1DE}(x_h; \omega)$ , depends only on the source-receiver offset ( $x_h$ ) and the frequency ( $\omega$ ). The Fourier transform over the 2D source data from a 1D earth can be shown as,

$$D(k_g, k_s; \omega) = \iint e^{ik_g x_g} e^{-ik_s x_s} D^{2D1DE}(x_h; \omega) dx_g dx_s \quad (5)$$

Rearranging the variables from  $(k_g, k_s)$  to  $(k_h, k_m)$  can give us,

$$D(k_h, k_m; \omega) = \frac{1}{2} \int e^{ik_h x_h} D^{2D1DE}(x_h; \omega) dx_h \int e^{ik_m x_m} dx_m = 2\pi D^{2D1DE}(k_h; \omega) \delta(2k_m), \quad (6)$$

where  $k_h = \frac{k_g + k_s}{2}$  and  $k_m = \frac{k_g - k_s}{2}$ . The data is independent of  $x_m$  and can come out of the  $x_m$  integral. Consequently, the

Fourier transform integral over  $x_m$  can produce a Dirac delta function in  $k_m$ . Since the 2D source ISS FSME algorithm needs data in  $(k_g, k_s)$ , we can change the variables in equation (6) back to  $(k_g, k_s)$  as,

$$D(k_g, k_s; \omega) = 2\pi D^{2D1DE}(k_g; \omega) \delta(k_g - k_s), \quad (7)$$

where  $k_g = k_s = k_m$  defined by the sifting property of the Dirac delta function.

As part of a complete dataset, the preprocessed data  $D'$  has the same symmetry as  $D$ , which is  $D'_n(k_g, k_s; \omega) = 2\pi D_n^{2D1DE}(k_g; \omega) \delta(k_g - k_s)$ . By applying this 1D earth data  $D'_n$  to equation (3), the algorithm becomes

$$D_n^{2D1DE}(k_h; \omega) = \frac{2}{i\rho_r B(\omega)} D_1^{2D1DE}(k_h; \omega) q D_{n-1}^{2D1DE}(k_h; \omega) e^{iq(\varepsilon_g + \varepsilon_s)}, \quad (8)$$

for  $n \geq 2$  and,

$$D^{2D1DE}(k_h, \omega) = \sum_{n=1}^{\infty} D_n^{2D1DE}(k_h; \omega), \quad (9)$$

where  $k_h = k_g = k_s$  (by evaluating the Dirac delta functions) and  $q = \text{sgn}(\omega) \sqrt{(\omega/c_0)^2 - k_h^2}$ . Free-surface multiple removed data in the space domain can be obtained by an inverse Fourier transform as,

$$D^{2D1DE}(x_h; \omega) = \frac{1}{2\pi} \int D^{2D1DE}(k_h; \omega) e^{ik_h x_h} dk_h. \quad (10)$$

The process following equations (8), (9) and then (10) gives us the ISS FSME algorithm assuming a 2D line source for a 1D subsurface.

### THE ISS FSME ALGORITHM ASSUMING A 3D POINT SOURCE FOR A 1D SUBSURFACE

3D data generated by a 1D earth depend only on the source-receiver offset and the frequency and has a spatial circular symmetry in cylindrical coordinates (independent of azimuth angle). This symmetry makes it convenient to study the 1D earth problem with cylindrical coordinates, which is characterized by a radial length, an azimuth angle and a vertical position. The 3D vectors  $(x, y, z)$  and  $(k_x, k_y, k_z)$  in Cartesian coordinates can be transformed to  $(r_i, \theta_i, z_i)$  and  $(k_{ri}, \phi_i, k_{zi})$ ,  $i \in \{g, 1, 2, s\}$ , in cylindrical coordinates. The dependence of 3D data for a 1D earth can be expressed as  $D^{3D1DE}(|\vec{r}_g - \vec{r}_s|, \omega)$  or  $D^{3D1DE}(r_h, \omega)$ , where  $\vec{r}_g$  and  $\vec{r}_s$  are the projections of receiver and source locations on to the x-y plane, respectively.  $r_h$  is the magnitude of the difference between  $\vec{r}_g$  and  $\vec{r}_s$ . Due to the cylindrical symmetry, the 3D source/1D subsurface data can be transformed to the  $(k_{ri}, \omega)$  domain as (Lin and Weglein, 2015b),

$$D(\vec{k}_g, \vec{k}_s; \omega) = D^{3D1DE}(k_{rh}; \omega) (2\pi)^2 \frac{\delta(k_{rg} - k_{rs}) \delta(\phi_g - \phi_s)}{k_{rg}}, \quad (11)$$

## Incorporating a 3D point source in the ISS FSME for a 1D subsurface and its influence on the subsequent processing

where  $k_{rh} = k_{rg}$ . The receivers are required along the  $r$ -direction in  $D^{3D1DE}(r_h; \omega)$ , because

$$D_1^{3D1DE}(k_{rh}; \omega) = 2\pi \int_0^\infty D^{3D1DE}(r_h; \omega) J_0(k_{rh}r_h) r_h dr_h. \quad (12)$$

The Dirac delta functions in equation (11) under cylindrical coordinates are equivalent to  $\delta(k_{xg} - k_{xs})\delta(k_{yg} - k_{ys})$  under Cartesian coordinates.

Substitute equation (11) into the full 3D ISS FSME algorithm in equation (1) and change the variables of integration  $dk_x dk_y$  to  $k_r dk_r d\phi$  to get the 3D source ISS FSME algorithm for a 1D surface as,

$$D_n^{3D1DE}(k_{rh}; \omega) = \frac{2}{i\rho_r B(\omega)} D_1^{3D1DE}(k_{rh}; \omega) q D_{n-1}^{3D1DE}(k_{rh}; \omega) e^{iq(\varepsilon_g + \varepsilon_s)}, \quad (13)$$

for  $n \geq 2$  and

$$D^{3D1DE}(k_{rh}; \omega) = \sum_{n=1}^{\infty} D_n^{3D1DE}(k_{rh}; \omega), \quad (14)$$

where  $k_{rh} = k_{rg} = k_{rs}$  and  $q = \sqrt{(\frac{\omega}{c_0})^2 - k_{rh}^2}$ .  $D_n^{3D1DE}(k_{rh}; \omega)$  ( $n^{\text{th}}$ -order FS multiple prediction) or  $D^{3D1DE}(k_{rh}; \omega)$  (FS multiple removed data) need to be transformed back to the space domain by an inverse Hankel transform (derived from two dimension Fourier transform due to the independence of the azimuth angle), instead of an inverse Fourier transform. The free-surface multiple prediction  $D_n^{3D1DE}(r_h; \omega)$  can be obtained by using,

$$D_n^{3D1DE}(r_h; \omega) = \frac{1}{2\pi} \int_0^\infty D_n^{3D1DE}(k_{rh}; \omega) J_0(k_{rh}r_h) k_{rh} dk_{rh}. \quad (15)$$

Similarly, the FS multiple removed data can be transformed to the space-time domain by,

$$D^{3D1DE}(r_h; \omega) = \frac{1}{2\pi} \int_0^\infty D^{3D1DE}(k_{rh}; \omega) J_0(k_{rh}r_h) k_{rh} dk_{rh}. \quad (16)$$

In an acquisition geometry where sources and receivers are on the same streamer in a 3D survey, we can take  $r$  along any angle in the  $x$ - $y$  plane, including  $r = x$ .

## NUMERICAL RESULTS

The synthetic 3D source data are generated based on acoustic layered models by using the reflectivity method with a limited bandwidth. All the datasets are pre-stack shot records without reference wave or ghost, which satisfies the prerequisites of the ISS FSME algorithm.

### Examine the significance of matching the source dimension

To show the significance of matching the source dimension in data and processing, we designed model I in figure 1 (a) to synthesize a 3D source data, which is shown in figure 1 (b). The data contains two primaries and two isolated free-surface multiples. Figure 2 presents the ISS free-surface multiple prediction results with different assumptions of source dimension.

The top figures in (a) and (b) show the results in shot gather, and the bottom wiggle plots in (a) and (b) give the comparison between data (blue line) and free-surface multiple prediction (dashed red line).

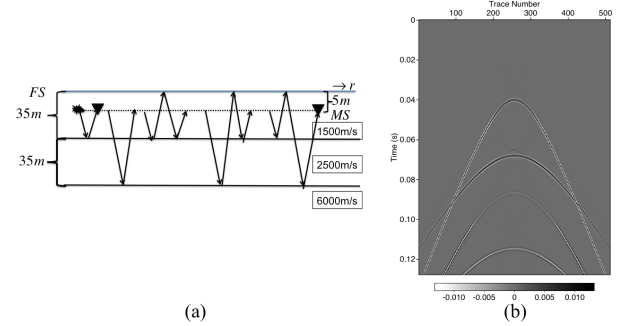


Figure 1: (a) Acoustic model I and (b) synthetic 3D point source data based on model I.

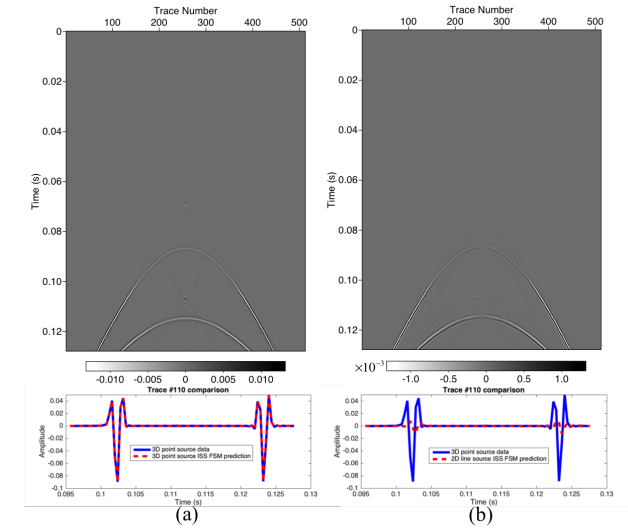


Figure 2: Free-surface multiple prediction (a) assuming a 3D point source and (b) assuming a 2D line source.

When the source dimension in processing matches the data, as shown in figure 2 (a), the prediction result provides the accurate time and exact amplitude of free-surface multiples. The wiggle comparison illustrates that the events predicted by the ISS FSME algorithm assuming a 3D point source (dashed red line) carry the same wavelet shape and amplitude as the free-surface multiples in the data (blue line). After simply subtracting (a) from data, the free-surface multiples can be completely removed.

In contrast to the 3D source prediction, the 2D line source prediction (figure 2 (b)) can generate deviated wavelet and much smaller amplitude (dashed red line) than the original free-surface multiples (blue line). To show this prediction, we applied a  $10^{-1}$  smaller scale color bar to make the shot gather visible. In this case, subtracting the prediction from the data can produce free-surface multiple residues, which are harmful

## Incorporating a 3D point source in the ISS FSME for a 1D subsurface and its influence on the subsequent processing

to subsequent processing (e.g. ISS internal multiple attenuation/elimination). Generally, the energy minimization criterion will be applied in this situation to make the subtraction effective, which is known as adaptive subtraction. And indeed the adaptive method works well when the events in the data are isolated. However, when the primaries and multiple are overlapping, the energy minimization criterion can fail to remove the multiples without harming the primaries.

### Examine the consequence of mismatching the source dimension in FSM removal on subsequent processing

The second test is performed to examine the consequence of mismatching the source dimension in one processing step to the next step. The model II in figure 3 (a) is used to generate synthetic 3D point source data (figure 3 (b)). This dataset contains two primaries, three free-surface multiples and one internal multiple, which is processed by ISS FSM removal and continued ISS internal multiple prediction. Figure 4 (a) and (b) present the free-surface multiple removed result in left panel and the internal multiple prediction result in right panel. Both of the internal multiple prediction (right panels in figure 4 (a) and (b)) results assume a 3D point source.

Left panel in figure 4 (a) shows the ISS FSM removed result assuming a 3D point source, which matches the source dimension in the synthetic data. This result indicates that incorporating a 3D source in algorithm can completely remove the FSM, which produces a satisfactory prerequisite of subsequent ISS internal multiple attenuation algorithm. Continued 3D point source internal multiple prediction has been shown in the right panel of figure 4 (a). The red arrow is pointed to the predicted internal multiple event. The internal multiple prediction works well as an attenuator, which provides accurate time and approximate amplitude of the internal multiple event.

However, applying a frequently used 2D line source ISS FSME algorithm on a 3D point source data can make the prediction far from effective. The ISS FSM removed result assuming a 2D line source is shown in the left panel of figure 4 (b). Compared to the original data shown in figure 3 (b), the FSM residues present in the result after FSM removal. The right panel of figure 4 (b) shows the internal multiple prediction using the source-dimension-mismatched FSM removed result (left panel) as input. If the residues of FSM exist in the input of subsequent ISS internal multiple attenuation, several artifacts can occur in the internal multiple prediction. The artifacts can be cataloged as (1) false events (pointed by green arrows), (2) events sitting on the FS multiple residues (pointed by blue arrows), and (3) events sitting on the internal multiple prediction (pointed by yellow arrow). The causes of artifacts have been discussed in Lin and Weglein (2015a).

## CONCLUSION

In this abstract, a new 3D source ISS free-surface-multiple-elimination algorithm has been proposed for a 1D subsurface. The numerical results demonstrate that the modified algorithm can eliminate the free-surface multiple events for one 3D shot gather. For a data set with a 3D source and a 1D subsurface,

using a 2D line source ISS FSME algorithm can produce a much less effective prediction. Furthermore, the subsequent ISS internal multiple prediction depends on the success of free-surface multiple removal. The results show that using input data with free-surface multiple residues can produce significant artifacts in the subsequent ISS internal multiple attenuation algorithm. Therefore, any step/prerequisite that cannot be carried out effectively can lead to negative consequences for subsequent processing. In this paper, we demonstrate that incorporating a 3D source in a 1D ISS free-surface elimination algorithm is an important factor for predicting free-surface multiples and on subsequent processing steps and objectives.

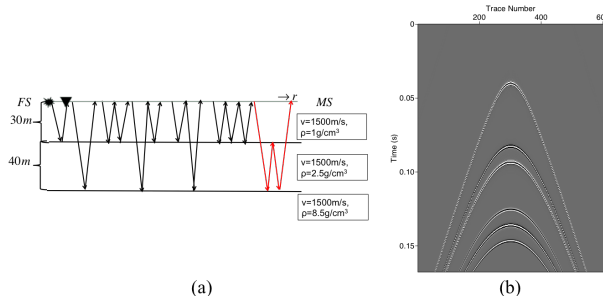


Figure 3: (a) Acoustic model II and (b) synthetic 3D point source data based on model II.

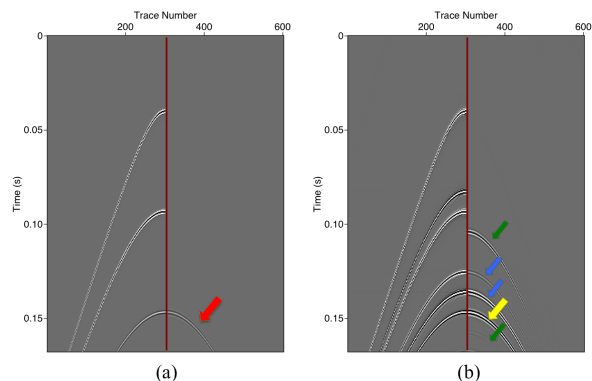


Figure 4: (a) Comparison between 3D point source ISS FSME result (left panel) and continued 3D point source ISS internal multiple prediction (right panel) using the result in left panel as input; (b) Comparison between 2D line source ISS FSME result (left panel) and continued 3D point source ISS internal multiple prediction (right panel) using the result in left panel as input.

## ACKNOWLEDGMENTS

We are grateful to all the M-OSRP sponsors for their long-term support and encouragements.